

# Equation of state of paramagnetic CrN from *ab initio* molecular dynamics

Peter Steneteg,\* Björn Alling, and Igor A. Abrikosov

*Department of Physics, Chemistry, and Biology (IFM), Linköping University, SE-581 83 Linköping, Sweden*

(Received 6 October 2011; revised manuscript received 2 February 2012; published 5 April 2012)

The equation of state for chromium nitride has been debated in the literature in connection with a proposed collapse of its bulk modulus following the pressure-induced transition from the paramagnetic cubic phase to the antiferromagnetic orthorhombic phase [F. Rivadulla *et al.*, *Nature Mater.* **8**, 947 (2009); B. Alling *et al.*, *ibid.* **9**, 283 (2010)]. Experimentally the measurements are complicated due to the low transition pressure, while theoretically the simulation of magnetic disorder represents a major challenge. Here a *first-principles* method is suggested for the calculation of thermodynamic properties of magnetic materials in their high-temperature paramagnetic phase. It is based on *ab initio* molecular dynamics and simultaneous redistributions of the disordered but finite local magnetic moments. We apply this disordered local moments molecular dynamics method to the case of CrN and simulate its equation of state. In particular the debated bulk modulus is calculated in the paramagnetic cubic phase and is shown to be very similar to that of the antiferromagnetic orthorhombic CrN phase for all considered temperatures.

DOI: 10.1103/PhysRevB.85.144404

PACS number(s): 75.10.-b, 75.20.En, 75.20.Hr, 71.15.Pd

## I. INTRODUCTION

Chromium nitride is a material which combines practical and industrial relevance as a component in protective coatings<sup>1,2</sup> with fascinating fundamental physical phenomena. The latter include a phase transition with a magnetically driven lattice distortion<sup>3</sup> between an antiferromagnetic orthorhombic low-temperature phase and a paramagnetic cubic high-temperature phase.<sup>4</sup> The importance of strong electron correlations as well as the necessity to model the paramagnetic state using finite disordered local moments have been recently shown.<sup>5,6</sup> Important issues, such as the impact of the phase transition on the compressibility of the material<sup>7,8</sup> as well as on the electrical conductivity<sup>9,10</sup> are still subjects of an intense discussion.

The core problem of obtaining a complete understanding of these phenomena and properties on the most fundamental level of physics arises from the difficulty of simulating the paramagnetic high-temperature phase from first principles. In this work we first discuss the methodologies that have been used in theoretical treatments of paramagnetism. Then we present a practical scheme for calculating thermodynamic properties, in particular the equation of state, of a paramagnetic material at elevated temperature merging *ab initio* molecular dynamics (MD) and the disordered local moments model (DLM). This DLM-MD technique is then applied to investigate the influence of temperature and pressure on the compressibility of CrN. We show that the change of the bulk modulus of CrN upon the pressure-induced phase transition is minimal, strengthening conclusions from earlier static calculations<sup>6,8</sup> which questioned its reported collapse.<sup>7</sup>

## II. MODELING THE PARAMAGNETIC STATE

### A. Background

A theory that describes the finite-temperature aspects of itinerant electron magnets has to take into account the existence of local magnetic moments present above the magnetic transition temperature, the Curie temperature  $T_C$  or the Néel temperature  $T_N$  for a ferromagnetic or an antiferromagnetic

material, respectively.<sup>11</sup> At the same time, the majority of methods used for *ab initio* electronic structure calculations nowadays are based on the density functional theory (DFT) in the local (local spin density, LSDA) or semilocal (generalized gradient, GGA) approximations. While they are known to give an accurate description of the ground state properties of magnetic systems,<sup>12</sup> its straightforward generalization to finite temperatures leads to quantitative as well as qualitative errors.<sup>13</sup> Indeed,  $T_C$  of transition metals are overestimated by a factor of five and there are no moments and no Curie-Weiss law above  $T_C$ . A solution to this problem should in principle be sought in the physics of strongly correlated electron systems. In particular, the dynamical mean-field theory (DMFT),<sup>14</sup> combined with LDA band structure calculations, has been used with success for simulations of finite-temperature magnetism in Fe and Ni.<sup>15</sup> However, its application to the study of the structural phase transition in Fe<sup>16</sup> had to neglect a contribution from the lattice dynamics, because of prohibitively high computational cost and difficulties in calculating forces between atoms.<sup>17</sup>

At the same time, it is realized that LSDA calculations at zero temperature can provide valuable information for the description of the finite temperature magnetism. One way of doing this is to extract magnetic interactions in the form of exchange constants for a classical Heisenberg model<sup>18</sup> or magnetic “forces” (the first variation of the total energy for a differential rotation of a local moment)<sup>19,20</sup> from DFT calculations and to use them in statistical mechanics<sup>21–25</sup> or in spin dynamics<sup>26,27</sup> simulations of magnetic properties at elevated temperatures.

Another useful approach is given by the so-called disordered local moment model, introduced by Hubbard<sup>28–30</sup> and Hasegawa<sup>31,32</sup> and combined with the LSDA-DFT by Gyorfyy *et al.*<sup>13</sup> Within the DLM picture, the local magnetic moments exist in the paramagnetic state above the magnetic transition temperature, but are fully disordered. The magnetically disordered state can be described as a pseudoalloy of equal amounts of atoms with spin up and spin down orientations of their magnetic moments, and its electronic structure and the total

energy can be calculated within the conventional alloy theory using the coherent potential approximation (CPA)<sup>13</sup> or the supercell technique.<sup>6</sup> Still, to the best of our knowledge all the applications of the DLM model so far have neglected the effect of lattice vibrations.

On the other hand, the importance of lattice dynamics for an accurate description of thermodynamic properties of materials is well recognized by now.<sup>33,34</sup> The effect of lattice vibrations should be included in the description of the paramagnetic state of magnetic materials, as it occurs only at elevated temperatures. However, simultaneous treatment of the magnetic disorder, inherent to the paramagnetic state, and lattice vibrations represent a truly challenging task.

State-of-the-art treatments of lattice vibrations are based either on (quasi)harmonic calculations of the phonon dispersion relations or on molecular dynamics simulations.<sup>35</sup> For magnetically ordered materials these techniques can be applied straightforwardly. However, in the presence of magnetic excitations this will not work. In particular, in the paramagnetic state at high temperatures the relevant magnetic excitations are associated with spin flips. Their characteristic time scale can be estimated by the spin decoherence time  $t_{dc}$ . Spin dynamics simulations of the spin autocorrelation function in bcc Fe above  $T_C$ <sup>27</sup> show that  $t_{dc}$  is of the order of 20–50 fs. In materials with lower  $T_C$  it should be larger by approximately a corresponding factor, because both  $T_C$  and the velocity of the propagation of the local moments are related to the strength of the exchange interactions. At the same time a typical MD run should be carried out for at least 3–5 ps, as dictated by the inverse of the Debye frequency ( $\sim 10^{-12}$  s). This means that magnetic configurations should change often during the MD run. Simultaneously, a typical MD time step is of the order of 1 fs, which is still much smaller than  $t_{dc}$ . Thus, the magnetic degree of freedom is slow on the time scale relevant for the determination of temporal evolution of a particular atomic configuration, but fast on the time scale relevant for a proper exploration of the phase space of atomic configurations. Therefore, the adiabatic decoupling between magnetic and vibrational degrees of freedom cannot be applied, and they should be treated within one single framework. Similar arguments can be used to question the validity of lattice dynamics studies for paramagnetic materials based on a quasiharmonic approximation. Perhaps the most consistent approach to the analysis of spin-lattice interactions at finite temperature would be to apply a combination of molecular dynamics with *ab initio* spin dynamics<sup>20</sup> or with DMFT. However, at present such calculations are hardly feasible in practice.

Within our approach we describe the paramagnetic state of a system within the disordered local moment picture. In this approach, local moments exist at each magnetic site of a system (in our case, at Cr sites in CrN) and are commonly thought to fluctuate fairly independently. Thoughtful discussions of the DLM model can be found in Refs. 13,28,30–32 and 36. In a previous work,<sup>6</sup> we took one step toward the simultaneous modeling of magnetic and vibrational finite-temperature effects by suggesting two alternative supercell implementations of the DLM calculations, the special quasirandom structure (SQS)<sup>37</sup> methodology and a magnetic sampling method (MSM). In the MSM, the energies of a number of randomly

generated magnetic distributions were calculated and their running average was taken as the potential energy of the paramagnetic sample. In Ref. 6 it was shown that the two approaches give almost identical results.

Unfortunately, if the vibrations of atoms are to be included, one needs to go beyond the fixed magnetic state described by the SQS. The reason is that if a magnetic state is fixed in time one would see artificial static displacements of atoms off their lattice sites due to forces between the atoms with different orientations of their local moments and with different local magnetic environments. In the CrN case those are likely to be quite large due to the magnetic stress discussed in Ref. 3. In a real paramagnet, due to the time fluctuations of the local moments, these effects should be at least partially averaged out and suppressed depending on the time scales of the spin fluctuations and atomic motions.

The MSM could in principle be used to obtain the adiabatic approximation where the magnetic fluctuations are considered to be instantaneous on the time scales of atomic motions. This approximation would be obtained if the forces acting on each atom were averaged over a sufficient number of different magnetic samples during each time step of a molecular dynamics simulation. The obvious drawback in this approach is that a large number of calculations needs to be run in parallel, probably leading to two orders of magnitude increase in computational efforts. Furthermore, as stated above it is not at all clear that this adiabatic approximation is motivated in any system. However, the MSM gives us a very good starting point for the implementation of the DLM picture in a MD framework.

## B. Disordered local moments molecular dynamics

In this work we introduce a method for molecular dynamics simulations of paramagnetic materials within the traditional *ab initio* MD framework. Starting from the DLM idea of a spatial disorder of local moments, we also change the magnetic state periodically and in a stochastic manner during our MD simulation. In this way we deal with a magnetic state that does not show order either on the length scales of our supercell or the time scale of our simulation. We make an approximation that the magnetic state of the system is completely randomly rearranged with a time step given by a spin flip time ( $\Delta t_{sf}$ ), and with a constraint that the net magnetization of the system should be zero. Hence to simulate a paramagnetic system with a spin flip time  $\Delta t_{sf}$ , we initialize our calculations by setting up a supercell where collinear local moments are randomly oriented and the total moment of the supercell is zero, and run collinear spin-polarized MD for the number of MD time steps ( $\Delta t_{MD}$ ) corresponding to the spin flip time, that is, for  $\Delta t_{sf} / \Delta t_{MD}$  time steps. Thereafter the spin state is randomized again, while the lattice positions and velocities are unchanged, and the simulation run continues.

Here it is worth pointing out that besides the treatment of the many-body effects important for the description of the paramagnetic state at the DLM-LSDA level,<sup>36</sup> or as will be discussed below for the present case DLM-LSDA +  $U$ , we introduce several additional approximations. In particular, we neglect effects due to noncollinear orientations of the local magnetic moments. This, however, is justified for the param-

agnetic state well above the magnetic transition temperature.<sup>13</sup> Note also that magnitudes of the local magnetic moments are allowed to vary as dictated by the self-consistent solution of the electronic structure problem at each step of the MD simulation. At the same time, we substitute the true spin dynamics with instantaneous modification of the sample magnetic structure with time steps  $\Delta t_{sf}$ . Here we follow Ref. 13 and make use of the physical picture that the simulated system, although ergodic, does not cover its phase space uniformly in time. In the DLM model one assumes that it gets stuck for long times, of the order of  $\Delta t_{sf}$ , near points characterized by a finite moment at every site pointing in more or less random directions and then moves rapidly (in our case instantly) to another similar point. The states of temporarily broken ergodicity are characterized by classical unit vectors  $e_i$  assigned to each site  $i$  and giving the direction of the magnetization averaged over the spatial extent of the  $i$ th site in the supercell and the time  $\Delta t_{sf}$ . The motion of temporarily broken ergodicity is mainly characterized by changes in the orientational configuration of the moments.

Note that in Ref. 13 the magnetic degree of freedom was related to an inverse spin-wave frequency  $t_{sw} \sim 1/\omega_{sw} \sim 100$  fs, which represents the dominating magnetic excitation at low temperatures. However, in the paramagnetic state at high temperatures the relevant magnetic excitations are associated with spin flips rather than with spin waves. Thus the relevant time scale is better characterized by the spin decoherence time  $\Delta t_{dc}$  rather than by the inverse spin-wave frequency. As we pointed out above, the latter was estimated to be of the order of 20–50 fs in bcc Fe above  $T_C$ .<sup>27</sup> For CrN, with a  $T_N$  around room temperature and probably with weaker exchange interactions, we expect that  $t_{dc}$  could be somewhat larger.

However, our procedure makes it possible to model a paramagnetic system for any particular time scale of the spin dynamics. In fact one can span the whole range between the static and adiabatic approximations: from the frozen magnetic structure to magnetic configurations that rearrange instantaneously on the time scales of each atomic motion during the MD run. Of course, the appropriate value of this parameter needs to be found with real spin dynamics calculations or taken from experiments. In this paper, we study a range of different spin flip times and their consequences for the obtained structural and thermodynamic properties of CrN.

### C. Computational details

All our first-principles calculations in this work are performed using the projector augmented wave (PAW) method<sup>38</sup> as implemented in the Vienna *Ab initio* Simulation Package (VASP).<sup>39–41</sup> The extended Lagrangian Born-Oppenheimer molecular dynamics method<sup>42</sup> and conventional Born-Oppenheimer molecular dynamics are used for simulations of the orthorhombic magnetically ordered and cubic magnetically disordered phases of CrN, respectively. The nitrogen  $2s$  and  $2p$  and Cr  $4s$  and  $3d$  states are treated as valence in the PAW pseudopotential. The electronic exchange-correlation effects are modeled using a combination of the local density approximation<sup>43</sup> with a Hubbard Coloumb term (LDA +  $U$ )<sup>44</sup> using the double-counting correction scheme suggested by Dudarev *et al.*<sup>45</sup> The value of the effective  $U$  ( $U^{\text{eff}} = U - J$ ) applied only to the Cr  $3d$  orbitals is taken

as 3 eV, found to be optimal from a comparison with several experimentally measured structural and electronic properties of CrN in Ref. 6.

Our simulation box, both for the cubic and orthorhombic phases, contains 32 Cr and 32 N atoms arranged in a supercell of  $2 \times 2 \times 2$  conventional unit cells. As demonstrated in Ref. 6, this supercell size is sufficient for an adequate description of the magnetic disorder in CrN. In the orthorhombic case, the primitive vectors of the supercell are tilted and scaled in line with the results of a structural optimization of this low-temperature antiferromagnetic phase.

The plane wave energy cutoff is set to 400 eV. We use a Monkhorst-Pack scheme<sup>46</sup> for sampling of the Brillouin zone using a grid of  $2 \times 2 \times 2$   $k$  points. To check the accuracy of the potential energies and pressures a selection of configurations is chosen out of the MD simulation run and recalculated with a higher accuracy. The error arising from the  $k$ -point sampling is relatively constant with a shift of about 35 meV and a standard deviation of less than 2 meV. Hence the relative potential energies that are calculated have a high accuracy. The pressures also have a small constant shift of about 0.2 GPa with a standard deviation less than 0.1 GPa when the electronic structure calculations are converged with respect to the  $k$ -points mesh.

The simulations are carried out using a canonical ensemble (NVT) in order to control the temperature of the simulation, avoid artificial energy drift, and minimize the influence of the particular choice of initial magnetic and lattice configurations in the simulations. We use the standard Nose thermostat<sup>47</sup> implemented in VASP, with the default Nose mass set by VASP. The values of the bulk modulus  $K_0$  have been determined by fitting our calculated pressure and volume data to the Birch-Murnaghan equation of state:<sup>48,49</sup>

$$P = 3K_0 f_E (1 + 2f_E)^{5/2} [1 + 2/3(K'_0 - 4)f_E], \quad (1)$$

where  $K_0$  is the bulk modulus at ambient pressure and  $K'_0$  is its derivative with respect to pressure. The Eulerian strain  $f_E$  is defined as  $f_E = 1/2[(V_0/V)^{2/3} - 1]$ , where  $V$  and  $V_0$  are the volume and equilibrium volume, respectively, at the corresponding temperature.

## III. APPLICATION TO CrN

### A. The potential energy

From the MD calculation we extract the potential energies of CrN, essentially the total energy with the kinetic energy of the ions subtracted. As can be seen in Fig. 1, the potential energy of the system is well conserved. To investigate the influence of the spin flip time, the potential energy of CrN is calculated for several  $\Delta t_{sf}$ . The results are shown in Fig. 1.

In Fig. 2 these potential energies are collected and shown relative to the potential energy of the calculations with shortest  $\Delta t_{sf}$ , 5 fs. There is a clear shift in potential energy of about 10 meV from the simulations with the shortest spin flip times of 5 fs to the longest of 100 fs. This can be compared with the total energy reduction due to static relaxations of 15 meV that we get by using the SQS approach treating the magnetic state as frozen in time. We note that for the lower values of  $\Delta t_{sf}$ , corresponding to fast spin decoherence, there is a plateau where the potential energy is only weakly influenced by  $\Delta t_{sf}$ .

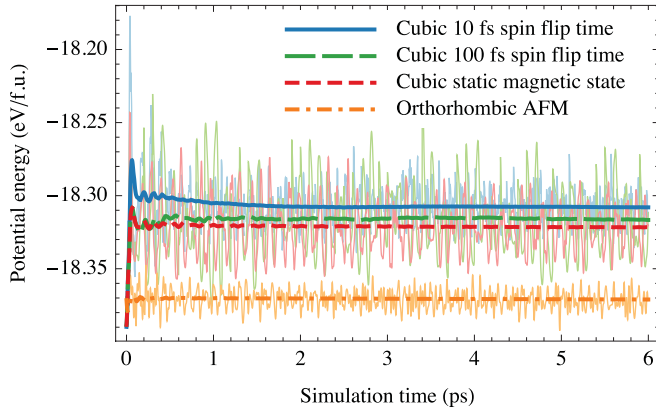


FIG. 1. (Color online) Potential energy of cubic paramagnetic CrN as a function of simulation time calculated at 300 K using DLM-MD method. Shown are the results obtained with a spin flip time of 10 fs and 100 fs, as well as with a frozen magnetic state. Results for conventional MD simulations carried out for CrN in the orthorhombic antiferromagnetic ground state are also shown for comparison. The potential energy is stable and well converged as can be seen by the included running averages (thick lines).

However, between spin flip times of 15 and 50 fs, there is a considerable change in potential energy. Of course, the energy scale should be material specific.

We suggest, as a quick test of how important to consider this effect, a calculation of relaxation energies of a paramagnetic system using the SQS approach<sup>6</sup> with a fixed magnetic state through the relaxation. The obtained relaxation energy should correspond to an upper limit on the potential energy dependence on  $\Delta t_{sf}$ .

### B. Magnetic moments

In Fig. 3 we analyze the evolution of the magnetic structure during the DLM-MD simulations of the cubic phases of CrN at 300 K, and compare it with conventional MD simulations of magnetically ordered orthorhombic phase. It is seen that during all the simulations the magnetic moments propagate in a controlled manner. The magnitude of Cr local magnetic

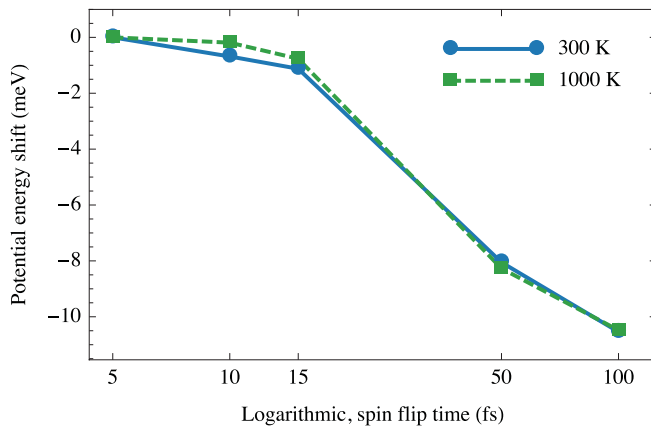


FIG. 2. (Color online) Potential energy shift calculated for paramagnetic CrN as a function of the spin flip time  $\Delta t_{sf}$ . The shortest spin flip time of 5 fs is taken as reference.

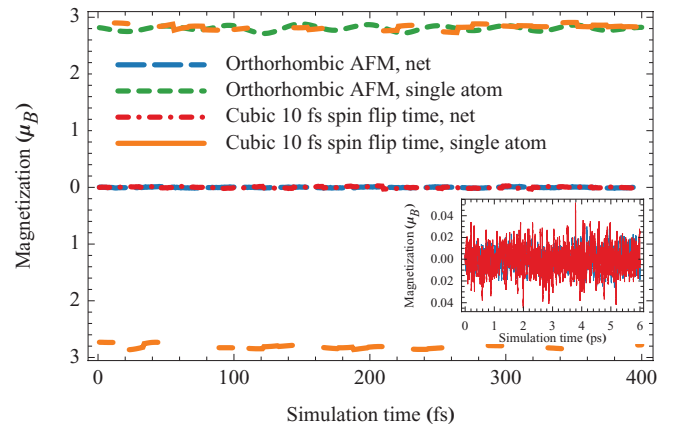


FIG. 3. (Color online) Evolution of the net magnetic moment averaged per supercell and local moment of one Cr atom for the orthorhombic and cubic phases at 300 K during the first 400 fs of the simulation. For the cubic phase the DLM spin configuration is changed every 10 fs. The behavior shown here is typical for the entire simulation, as well as for other simulated temperatures and spin flip times. The inset demonstrates small fluctuations of the net magnetic moment during the entire simulation.

moments is stable in all our calculations. The total magnetic moment per supercell is practically conserved and fluctuates about zero during the whole simulation run for both AFM-orthorhombic CrN and DLM-MD simulations of paramagnetic cubic CrN. The inset in Fig. 3 magnifies the fluctuations and confirms that we obtain a rather accurate description of the magnetically disordered state with nearly vanishing net magnetic moment during the whole simulation run. In addition, we show in Fig. 3 time evolution of a magnetic moment on one arbitrary chosen Cr atom during the first 400 fs in a DLM-MD with  $\Delta t_{sf} = 10$  fs, as well as in the orthorhombic AFM structure. There are almost no changes in the amplitude of the moment, indicating that we are dealing with a very good Heisenberg system. Moreover, the moment does not flip during time  $\Delta t_{sf}$  between the deliberate rearrangements of the supercell magnetic structure in our DLM-MD simulations.

### C. Pair distances

In order to analyze the difference between the proposed DLM-MD simulations and magnetostatic MD in more details, an investigation of the local environment of the different atoms is carried out, especially the Cr-Cr metal nearest neighbor distances. In Fig. 4 histograms are shown of all the Cr-Cr nearest neighbor distances. These are also separated into  $\uparrow\uparrow$ ,  $\downarrow\downarrow$  and  $\uparrow\downarrow$ ,  $\downarrow\uparrow$  pairs. Hence we can see the effect of the magnetic state on the distribution of pair distances. In Fig. 4(a) the  $\Delta t_{sf}$  is very short, 10 fs; hence the atoms do not have time to adjust their positions for the current orientation of local magnetic moments and we do not see any difference in distances between the  $\uparrow\uparrow$ ,  $\downarrow\downarrow$  and the  $\uparrow\downarrow$ ,  $\downarrow\uparrow$  pairs. In Fig. 4(b), the spin flip time is increased to 100 fs and now the atoms have had sufficient time to move toward the energetically preferential positions. Consequently, a shift in pair distances between  $\uparrow\uparrow$ ,  $\downarrow\downarrow$  and  $\uparrow\downarrow$ ,  $\downarrow\uparrow$  is evident. Fig. 4(c) is obtained with the same orientation of local moments during the whole MD run. Here we also see a splitting in the pair distances

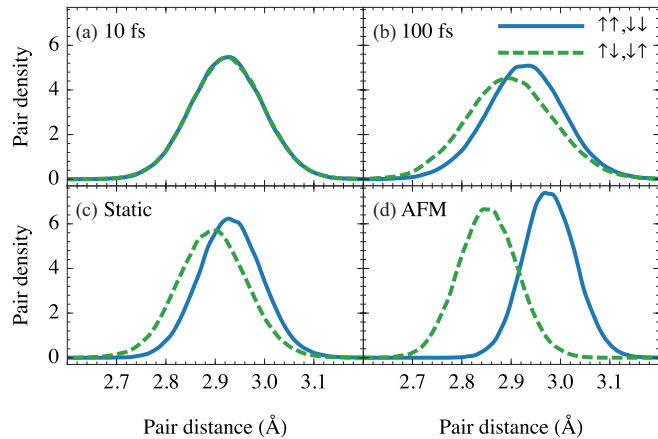


FIG. 4. (Color online) Histogram of the Cr-Cr nearest neighbor distances for Cr atoms with parallel (solid line) and antiparallel (dashed line) orientations of local magnetic moments obtained from DLM-MD simulation for the cubic paramagnetic phase at 300 K. (a)  $\Delta t_{sf} = 10$  fs. (b)  $\Delta t_{sf} = 100$  fs. (c) Static magnetic state. (d) The orthorhombic antiferromagnetic phase of CrN calculated with conventional *ab initio* MD for comparison.

between the  $\uparrow\uparrow$ ,  $\downarrow\downarrow$  and the  $\uparrow\downarrow$ ,  $\downarrow\uparrow$  pairs, which is of the same order as in the previous case. Hence, 100 fs between the rearrangement of magnetic configurations is long enough for the atomic nuclei to adjust considerably their positions in the supercell to the given magnetic configuration. In the last figure, Fig. 4(d), the pair distances are shown for the low-temperature antiferromagnetic orthorhombic ground state for comparison. Here the  $\uparrow\uparrow$ ,  $\downarrow\downarrow$  and  $\uparrow\downarrow$ ,  $\downarrow\uparrow$  pairs of magnetic moments are arranged in an ordered way—see, e.g., Fig. 4 in Ref. 6—that allows for maximal relaxation of atomic coordinates in combination with a structural relaxation of the unit cell, giving rise to a large separation between the two different kinds of pairs.

A possibility of statistical correlations between the atomic distances and the orientation of atomic moments also in a dynamically changing paramagnetic phase is indeed an intriguing thought experiment. Although we cannot rule out its existence from principal considerations, to the best of our knowledge it has never been reported in experiments. However, we note that our two main approximations in the present DLM-MD, the usage of collinear moments and the temporarily broken ergodicity of the DLM approach, are likely to introduce inaccuracies that exaggerate those local spin-lattice correlations when a slow spin dynamics is modeled. Therefore, when the here suggested method is used, a smaller value of  $\Delta t_{sf}$ , corresponding to the absence of differences in distances between atoms with parallel and antiparallel local moments, like in Fig. 4(a), should be recommended. The presence of an energy plateau in Fig. 2 seems to indicate that this should be a reasonable approach.

#### D. Equation of state of CrN

Our main goal with this work is to study the equation of states, and in particular the bulk modulus of paramagnetic CrN which has recently been discussed in the literature.<sup>7,8</sup> Using our DLM-MD approach we are able to calculate volume as a function of temperature and pressure for both the paramagnetic cubic and the antiferromagnetic orthorhombic phases. In the

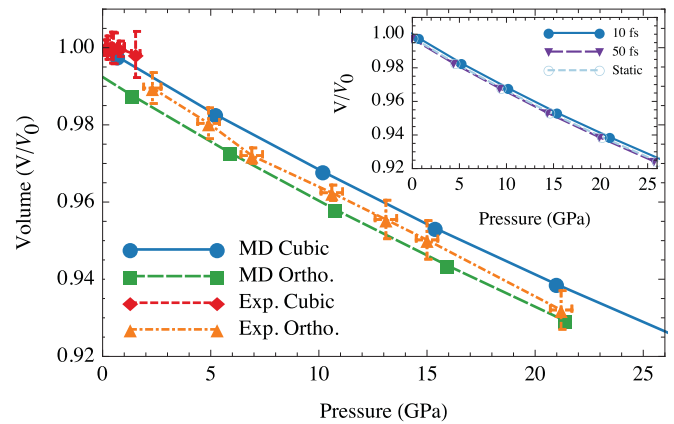


FIG. 5. (Color online) Volume as a function of pressure for the cubic and orthorhombic phase from MD simulations at 300 K. The equation of state for the cubic phase is calculated using a spin flip time of 10 fs. The calculated volumes are normalized with the calculated equilibrium volume ( $17.42 \text{ \AA}^3/\text{f.u.}$ ) of the cubic phase, and the experimental points (Ref. 7) with the measured equilibrium volume ( $17.84 \text{ \AA}^3/\text{f.u.}$ ) of the cubic phase. The inset shows the dependence on spin flip time for the calculated equation of state.

former case we also investigate whether there is an impact of the value of the spin flip time parameter on the equation of state. Thus we are able to investigate how both the dynamical change of magnetic configurations in the paramagnetic state and the lattice vibrations, neglected in previous theoretical works but of course present in the experiments, impact on the compressibility. Figure 5 shows the calculated volume as a function of pressure for the two phases at 300 K and compares them to the experimental measurements by Rivadulla *et al.*<sup>7</sup> One sees very good agreement between theoretical and experimental equations of state. In particular the relative shift in volumes between the two phases is reproduced within the measured error bars. The calculated slope of the orthorhombic phase agrees well with the measured values for this phase where the measurement is done over a large pressure range. The inset in Fig. 5 shows the influence of the spin flip time on the volume versus pressure curves in paramagnetic cubic CrN. A change in  $\Delta t_{sf}$  introduces a small shift of the volumes, but does not influence the slope of the curves.

In Table I we summarize calculated ground state parameters, equilibrium volumes  $V_0$  and bulk moduli  $K_0$ , obtained in our MD simulations for paramagnetic cubic and antiferromagnetic orthorhombic phases of CrN. They are also compared to our static calculations at zero temperature, as well as with theoretical calculations and experiment from the literature. Our calculated equilibrium volumes increase with temperature, indicating that the effect of thermal expansion is included in our simulations self-consistently. For both phases they agree well with experiment, within 2.5%, which is typical accuracy for first-principles simulations. We note in passing that slightly different values between  $V_0$  obtained in this work and in Ref. 8 are due to different values of parameter  $U$ , 3 eV and 4 eV, respectively. Though the latter gives better agreement with experiment for  $V_0$ , and consequently for  $K_0$ , the former gives more consistent description of all structural and electronic properties of CrN,<sup>6</sup> and we prefer to use it here.

TABLE I. Calculated equilibrium volume  $V_0$  ( $\text{\AA}^3/\text{f.u.}$ ) and bulk modulus  $K_0$  (GPa) of CrN in the orthorhombic antiferromagnetic and the cubic paramagnetic phases obtained at ambient pressure and at temperatures 0, 300, and 1000 K, respectively.

Method	Structure	Orthorhombic AFM		Cubic PM	
		$V_0$	$K_0$	$V_0$	$K_0$
Theory This work LDA + $U$ $U = 3$ eV	Static, 0 K	17.21	290	17.39	299
	DLM-MD 300 K	17.29	286	17.42	290
	DLM-MD 1000 K	17.50	261	17.59	269
Theory Ref. 8	Static, 0 K GGA	17.56	255	17.85	252
	Static, 0 K LDA + $U$ $U = 4$ eV	17.78	272	17.96	277
Theory Ref. 7	Static, 0 K GGA		255		340 <sup>a</sup>
	Static, 0 K LDA		260		430 <sup>a</sup>
Exp. Ref. 7	300 K	17.75	243–260	17.84	

<sup>a</sup>Nonmagnetic calculation.

However, the choice of  $U$  does not affect a comparison between ground state parameters of two phases of CrN. In particular, the volume difference between the cubic and orthorhombic structures is very well reproduced in our simulations.

Our results confirm the possibility of a pressure-induced phase transition from the cubic paramagnetic to the orthorhombic antiferromagnetic phase due to the slightly smaller volume of the latter, in line with previous investigations. Importantly, as can be seen in Table I and from the slopes of the curves in Fig. 5, the bulk modulus is found to be very similar between the two phases. This is the case both at 300 K, 1000 K, and in the static 0 K calculations yielding small differences as seen in previous work.<sup>8</sup> The calculations of the orthorhombic low-temperature phase at 1000 K is of course not of relevance for any comparison with experiments, but is included to show with certainty that temperature-induced vibrations are not influencing the *difference* in bulk modulus between the phases. At  $T = 300$  K and  $P = 0$  GPa we find  $K_0^{\text{para}} = 290$  GPa while  $K_0^{\text{AFM}} = 286$  GPa. This gives an insignificant difference of 4 GPa, far from the collapse of 25% or 85 GPa suggested in Ref. 7 to follow the transition from cubic to orthorhombic structures. A variation of the time between the rearrangement of the magnetic configurations does not influence the value of the bulk modulus in any appreciable way. Thus, explicit considerations of temperature-induced magnetic fluctuations and lattice vibrations do not change the main conclusions from previous works:<sup>6,8</sup> There is no theoretical support for a collapse of the bulk modulus of CrN upon the pressure-induced phase transition.

#### IV. SUMMARY

We present a method for calculation of thermodynamic properties of magnetic materials in their high-temperature

paramagnetic state. We use *ab initio* molecular dynamics and simulate the paramagnetic state with disordered nonvanishing local magnetic moments. Random configurations of the local moments in the simulation cell are switched at predetermined time intervals. Hence we can capture the influence of the dynamically disordered magnetic state on the lattice dynamics as it develops during the simulation. We apply this method to CrN which is known to have a strong interaction between the magnetic state and the lattice. We find that there is a connection between how fast the local moments are allowed to flip and the calculated potential energy. If the spin flip time is short,  $\sim 10$  fs, the lattice does not have time to respond, but if the spin flip time is increased to about 100 fs then the atomic positions start to show clear relaxation effects. We apply this disordered local moments molecular dynamics method to the calculation of the equation of state of paramagnetic cubic CrN and compare with calculations for the orthorhombic antiferromagnetic phase and with experiments. In particular we calculate the debated bulk modulus and find that there is only a very small difference, and definitely no collapse, in  $K_0$  between the orthorhombic antiferromagnetic phase and the cubic paramagnetic phase.

#### ACKNOWLEDGMENTS

We gratefully acknowledge financial support by the Swedish Research Council (VR) grant 621-2011-4426 and 621-2011-4417, and the Swedish Foundation for Strategic Research (SSF) Program SRL grant 10-0026 for this work, as well as Olle Hellman for fruitful discussions. The simulations were carried out using supercomputer resources provided by the Swedish National Infrastructure for Computing (SNIC).

\*peter.steneteg@liu.se

<sup>1</sup>J. Vetter, *Surf. Coat. Technol.* **76-77**, 719 (1995).

<sup>2</sup>A. E. Reiter, V. H. Derflinger, B. Hanselmann, T. Bachmann, and B. Sartory, *Surf. Coat. Technol.* **200**, 2114 (2005).

<sup>3</sup>A. Filippetti and N. A. Hill, *Phys. Rev. Lett.* **85**, 5166 (2000).

<sup>4</sup>L. M. Corliss, N. Elliott, and J. M. Hastings, *Phys. Rev.* **117**, 929 (1960).

<sup>5</sup>A. Herwadkar and W. R. L. Lambrecht, *Phys. Rev. B* **79**, 035125 (2009).

<sup>6</sup>B. Alling, T. Marten, and I. A. Abrikosov, *Phys. Rev. B* **82**, 184430 (2010).

<sup>7</sup>F. Rivadulla, M. Banobre-Lopez, C. Quintela, A. Pineiro, V. Pardo, D. Baldomir, M. Lopez-Quintela, J. Rivas, C. Ramos, H. Salva, J.-S. Zhou, and J. Goodenough, *Nature Mater.* **8**, 947 (2009).

<sup>8</sup>B. Alling, T. Marten, and I. Abrikosov, *Nature Mater.* **9**, 283 (2010).

- <sup>9</sup>P. A. Bhohe, A. Chainani, M. Taguchi, T. Takeuchi, R. Eguchi, M. Matsunami, K. Ishizaka, Y. Takata, M. Oura, Y. Senba, H. Ohashi, Y. Nishino, M. Yabashi, K. Tamasaku, T. Ishikawa, K. Takenaka, H. Takagi, and S. Shin, *Phys. Rev. Lett.* **104**, 236404 (2010).
- <sup>10</sup>X. Y. Zhang, J. S. Chawla, B. M. Howe, and D. Gall, *Phys. Rev. B* **83**, 165205 (2011).
- <sup>11</sup>T. Moriya, *Spin Fluctuations in Itinerant Electron Magnetism* (Springer-Verlag, Berlin, 1985).
- <sup>12</sup>P. James, O. Eriksson, B. Johansson, and I. A. Abrikosov, *Phys. Rev. B* **59**, 419 (1999).
- <sup>13</sup>B. L. Gyorffy, A. J. Pindor, J. Staunton, G. M. Stocks, and H. Winter, *J. Phys. F* **15**, 1337 (1985).
- <sup>14</sup>A. Georges, G. Kotliar, W. Krauth, and M. J. Rozenberg, *Rev. Mod. Phys.* **68**, 13 (1996).
- <sup>15</sup>A. I. Lichtenstein, M. I. Katsnelson, and G. Kotliar, *Phys. Rev. Lett.* **87**, 067205 (2001).
- <sup>16</sup>I. Leonov, A. I. Poteryaev, V. I. Anisimov, and D. Vollhardt, *Phys. Rev. Lett.* **106**, 106405 (2011).
- <sup>17</sup>G. Kotliar, S. Y. Savrasov, K. Haule, V. S. Oudovenko, O. Parcollet, and C. A. Marianetti, *Rev. Mod. Phys.* **78**, 865 (2006).
- <sup>18</sup>A. I. Liechtenstein, M. I. Katsnelson, V. P. Antropov, and V. A. Gubanov, *J. Magn. Magn. Mater.* **67**, 65 (1987).
- <sup>19</sup>V. P. Antropov, M. I. Katsnelson, M. van Schilfgaarde, and B. N. Harmon, *Phys. Rev. Lett.* **75**, 729 (1995).
- <sup>20</sup>V. P. Antropov, M. I. Katsnelson, B. N. Harmon, M. van Schilfgaarde, and D. Kusnezov, *Phys. Rev. B* **54**, 1019 (1996).
- <sup>21</sup>N. M. Rosengaard and B. Johansson, *Phys. Rev. B* **55**, 14975 (1997).
- <sup>22</sup>A. V. Ruban, S. Shallcross, S. I. Simak, and H. L. Skriver, *Phys. Rev. B* **70**, 125115 (2004).
- <sup>23</sup>A. V. Ruban, S. Khmelevskiy, P. Mohn, and B. Johansson, *Phys. Rev. B* **75**, 054402 (2007).
- <sup>24</sup>B. Alling, A. V. Ruban, and I. A. Abrikosov, *Phys. Rev. B* **79**, 134417 (2009).
- <sup>25</sup>B. Alling, *Phys. Rev. B* **82**, 054408 (2010).
- <sup>26</sup>B. Skubic, J. Hellsvik, L. Nordström, and O. Eriksson, *J. Phys.: Condens. Matter* **20**, 315203 (2008).
- <sup>27</sup>J. Hellsvik, B. Skubic, L. Nordström, B. Sanyal, O. Eriksson, P. Nordblad, and P. Svedlindh, *Phys. Rev. B* **78**, 144419 (2008).
- <sup>28</sup>J. Hubbard, *Phys. Rev. B* **19**, 2626 (1979).
- <sup>29</sup>J. Hubbard, *Phys. Rev. B* **20**, 4584 (1979).
- <sup>30</sup>J. Hubbard, *Phys. Rev. B* **23**, 5974 (1981).
- <sup>31</sup>H. Hasegawa, *J. Phys. Soc. Jpn.* **46**, 1504 (1979).
- <sup>32</sup>H. Hasegawa, *J. Phys. Soc. Jpn.* **49**, 178 (1980).
- <sup>33</sup>A. van de Walle and G. Ceder, *Rev. Mod. Phys.* **74**, 11 (2002).
- <sup>34</sup>M. J. Gillan, D. Alfe, J. Brodholt, L. Vocadlo, and G. D. Price, *Rep. Prog. Phys.* **69**, 2365 (2006).
- <sup>35</sup>R. M. Martin, *Electronic Structure, Basic Theory, and Practical Methods* (Cambridge University Press, Cambridge, UK, 2004).
- <sup>36</sup>A. M. N. Niklasson, J. M. Wills, M. I. Katsnelson, I. A. Abrikosov, O. Eriksson, and B. Johansson, *Phys. Rev. B* **67**, 235105 (2003).
- <sup>37</sup>A. Zunger, S.-H. Wei, L. G. Ferreira, and J. E. Bernard, *Phys. Rev. Lett.* **65**, 353 (1990).
- <sup>38</sup>P. E. Blöchl, *Phys. Rev. B* **50**, 17953 (1994).
- <sup>39</sup>G. Kresse and J. Hafner, *Phys. Rev. B* **48**, 13115 (1993).
- <sup>40</sup>G. Kresse and J. Furthmüller, *Phys. Rev. B* **54**, 11169 (1996).
- <sup>41</sup>G. Kresse and J. Furthmüller, *Comput. Mater. Sci.* **6**, 15 (1996).
- <sup>42</sup>P. Steneteg, I. A. Abrikosov, V. Weber, and A. M. N. Niklasson, *Phys. Rev. B* **82**, 075110 (2010).
- <sup>43</sup>D. M. Ceperley and B. J. Alder, *Phys. Rev. Lett.* **45**, 566 (1980).
- <sup>44</sup>V. I. Anisimov, J. Zaanen, and O. K. Andersen, *Phys. Rev. B* **44**, 943 (1991).
- <sup>45</sup>S. L. Dudarev, G. A. Botton, S. Y. Savrasov, C. J. Humphreys, and A. P. Sutton, *Phys. Rev. B* **57**, 1505 (1998).
- <sup>46</sup>H. J. Monkhorst and J. D. Pack, *Phys. Rev. B* **13**, 5188 (1976).
- <sup>47</sup>S. Nosé, *Prog. Theor. Phys. Suppl.* **103**, 1 (1991).
- <sup>48</sup>F. Birch, *Phys. Rev.* **71**, 809 (1947).
- <sup>49</sup>F. D. Murnaghan, *Proc. Natl. Acad. Sci. USA* **30**, 244 (1944).